Sensors & Actuators: B. Chemical 426 (2025) 137057

Contents lists available at ScienceDirect

Sensors and Actuators: B. Chemical

journal homepage: www.elsevier.com/locate/snb

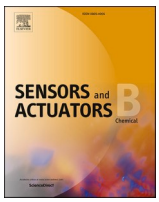

Carboxylesterase 2-based fluorescent probe with large Stokes shift for differentiating colitis from bowel cancer

Mo Ma [a,b], Siqi Zhang [b], Jingkang Li [b], Lihe Zhao [c], Daqian Song [b], Pinyi Ma [b,*], Xiangqun Jin [a,*]

[a] School of Pharmacy, Jilin University, Qianjin Street 2699, Changchun 130012, China
[b] College of Chemistry, Jilin Province Research Center for Engineering and Technology of Spectral Analytical Instruments, Jilin University, Qianjin Street 2699, Changchun 130012, China
[c] Shenzhen Experimental School, Niushan Road 768, Shenzhen 518000, China

ARTICLE INFO

Keywords:
Carboxylesterase 2 (CES2)
Fluorescent probe
Early diagnosis
Colitis
Colorectal cancer

ABSTRACT

Colitis is considered a significant risk factor for the development and progression of colorectal cancer due to excessive inflammation formed as a result of inflammatory bowel disease (IBD), which is linked to colorectal cancer development. Colorectal cancer often lacks overt symptoms in its early stages, leading to late-stage diagnosis in most patients. Therefore, timely diagnosis and differentiation of colitis and colorectal cancer are crucial. This study introduces a novel activatable carboxylesterase 2 (CES2) fluorescent probe, DBF-CES2, consisting of a cationic indolium fluorophore and a CES2-specific benzyl ester recognition group. The probe operates via the intramolecular charge transfer (ICT) mechanism. Upon binding and hydrolysis by CES2, a potent electron-donating hydroxyl group is released, enhancing the ICT effect and increasing fluorescence intensity, emitting red fluorescence light (λ_{em} = 680 nm). The probe had a large Stokes shift of 167 nm and a detection limit as low as 0.70 ng/mL. It also had high selectivity, sensitivity, and biocompatibility. Cellular imaging experiments demonstrated that CES2 expression levels in colorectal cancer cells were higher than those in normal cells. The DBF-CES2 probe specifically recognized endogenous CES2 in colorectal cancer cells, promptly distinguishing them from normal cells. *In vivo* imaging in mice confirmed that the probe could differentiate between colitis and colorectal cancer, allowing for the assessment of the therapeutic effects of two drugs. The synthesized CES2-targeting organic small molecule fluorescent probe DBF-CES2 is a new molecular tool for the early diagnosis of colitis and colorectal cancer-related diseases, holding significant potential in clinical diagnostics.

1. Introduction

Inflammatory bowel disease (IBD) represents a common gastrointestinal disorder, predominantly driven by immune dysfunction and microbial imbalance [1]. Characterized by symptoms like diarrhea, abdominal pain, and weight loss, and sometimes accompanied by oral ulcers and dermatitis, ulcerative colitis (UC)—which is a type of IBD—is a chronic inflammation primarily affecting the colonic mucosa [2–4]. Colitis, exacerbated by lifestyles and environmental factors, is increasingly recognized as a significant precursor for colorectal cancer, a malignancy known for its high morbidity and mortality due to its late-stage diagnosis [5–7]. Therefore, early diagnosis and differentiation of colitis and colorectal cancer are crucial.

Carboxylesterases (CES), particularly the CES1 and CES2 isoforms, play vital roles in the hydrolysis of drugs and xenobiotics in the liver and intestines, thereby influencing drug metabolism and detoxification processes [8–10]. CES2, which preferentially metabolizes compounds with larger hydroxyl and smaller acyl groups, emerges as a cancer biomarker due to its altered expression in various cancers, including colorectal cancer [11–15]. The ability to detect changes in CES2 expression is a promising avenue for early-stage disease diagnosis through advanced molecular imaging techniques such as fluorescence imaging [16–18]. Owing to its high sensitivity and specificity, and unique fluorescent properties, fluorescence imaging can be leveraged to detect and monitor dynamic biological processes to enable precise disease characterization at the molecular level [19–22]. Previous studies have reported the use of CES2-targeted fluorescent probes for diagnosing liver diseases [23–32]. For instance, Yin's group developed the probe JFast, which is an oxazine 1-based probe and responsive to CES2, to distinguish human primary liver cancer tissue from adjacent tissue

* Corresponding authors.
E-mail addresses: mapinyi@jlu.edu.cn (P. Ma), jinxq@jlu.edu.cn (X. Jin).

https://doi.org/10.1016/j.snb.2024.137057
Received 7 July 2024; Received in revised form 29 November 2024; Accepted 1 December 2024
Available online 2 December 2024

through significant fluorescence enhancement [33]. These results underscore the potential of JFast in clinical application and our understanding of the physiological and pathological processes related to hepatocellular carcinoma. Song's group developed a novel mitochondria-targeting near-infrared molecular imaging tool, YDT, for imaging and sensing CES2 during the early diagnosis of liver-related diseases [34]. Ma's group designed a selective, sensitive ratiometric endoplasmic reticulum-targeting CES2 fluorescent probe, ERNB, to monitor the activity and expression of CES2 in an acetaminophen-induced acute liver injury model [35]. However, their applications for intestinal diseases, especially colitis and colorectal cancer, are rarely reported [36–38].

This study presents the synthesis of a novel near-infrared small molecule fluorescent probe, DBF-CES2, tailored for the detection of CES2. In the probe's design, a donor-π-acceptor (D-π-A) structure with a benzyl ester as the CES2-specific recognition group was incorporated. Upon interacting with CES2, the probe undergoes hydrolysis, in turn triggering fluorescence emission that is indicative of the presence and activity of CES2. This probe had high selectivity and sensitivity, a large Stokes shift, good biocompatibility, and a low detection limit. In cellular imaging, DBF-CES2 was successfully applied to image endogenous CES2 in colorectal cancer cells and confirm the upregulation of CES2 expression in these cancer cells. *In vivo* imaging in mice demonstrated the probe's capability to distinguish between colitis and colorectal cancer and to assess the therapeutic effects of two drugs. The probe was developed to provide a non-invasive, highly sensitive diagnostic tool for the early detection and timely intervention of pathological changes. This work elucidates the role of CES2 in the pathogenesis of colitis and colorectal cancer, offering a more precise molecular target for future clinical diagnostics and treatment.

2. Experimental section

2.1. Organic synthesis

The synthesis process of DBF-OH and DBF-CES2 is described in Fig. 1.

2.1.1. DBF-OH synthesis

Under nitrogen protection, the synthesis began by combining 5-formyl-2-furanyl boronic acid (488 mg, 3 mmol), 4-iodophenol (438 mg, 2 mmol), potassium carbonate (828 mg, 6 mmol), and palladium acetate (31 mg, 0.14 mmol). The mixture was then added to 14 mL of 1,4-dioxane and 6 mL of deionized water, and then stirred overnight. Following this, the solvent was evaporated under reduced pressure. The resulting residue was purified by silica gel column chromatography using petroleum ether/ethyl acetate (10:1) as the eluent to yield a deep red solid powder denoted as compound 1 (202 mg). Next, compound 1 (160 mg, 0.53 mmol) and 3-ethyl-1,1,2-trimethyl-1H-benzo[*e*]indol-3-ium iodide (128 mg, 0.53 mmol) were dissolved in 10 mL of ethyl acetate and stirred until fully dissolved. After piperidine (53 μL, 0.53 mmol) was slowly added to the solution, the mixture was stirred at 85 °C for 12 h. The progress of the reaction was monitored by thin-layer chromatography (TLC). Upon completion of the reaction, the mixture was cooled to room temperature. The solvent was then removed under vacuum, and the final product was purified by silica gel column chromatography using CH_2Cl_2/CH_3OH (*v/v*, 100:1–20:1) as the eluent, which resulted in DBF-OH as a purple solid (204.8 mg, 65 % yield). ^{1}H NMR (600 MHz, DMSO-d_6) δ 10.24 (s, 1H), 8.46 – 8.33 (m, 2H), 8.27 (d, J = 8.9 Hz, 1H), 8.20 (d, J = 8.1 Hz, 1H), 8.08 (d, J = 9.0 Hz, 1H), 7.97 (d, J = 8.7 Hz, 2H), 7.83 – 7.74 (m, 1H), 7.75 – 7.65 (m, 2H), 7.34 – 7.21 (m, 2H), 6.95 (d, J = 8.7 Hz, 2H), 4.76 (q, J = 7.2 Hz, 2H), 2.00 (s, 6H), 1.51 (t, J = 7.2 Hz, 3H) (Figure S1). ^{13}C NMR (151 MHz, $CDCl_3$) δ 180.75, 164.84, 162.53, 160.96, 152.55, 137.94, 137.76, 133.93, 133.51, 131.70, 130.28, 129.14, 128.71, 127.60, 127.33, 127.10, 125.90, 122.74, 111.60, 53.52, 43.46, 27.06, 14.81 (Figure S2). HR-MS (*m/z*): Calculated for $[C_{28}H_{32}N_4O_5]^+$: 408.1959, found: 408.1908 (Figure S3).

2.1.2. DBF-CES2 synthesis

DBF-OH (118 mg, 0.2 mmol) was dissolved in 5 mL of CH_2Cl_2, followed by the addition of triethylamine (0.25 mmol). Benzoyl chloride (0.2 mmol, mixed with 1 mL CH_2Cl_2) was then added dropwise at 0 °C, and the mixture was stirred for 1 h. The reaction was incubated overnight at room temperature. The progress of the reaction was monitored using TLC. After the reaction was complete, the solvent was removed under reduced pressure, and excess benzoyl chloride was washed with petroleum ether. Finally, the product was purified by silica gel column chromatography using CH_2Cl_2/CH_3OH (*v/v*, 20:1) as the eluent; and the probe DBF-CES2 as a red solid (42 mg, 41 % yield) was obtained. ^{1}H NMR (600 MHz, $CDCl_3$) δ 8.28 – 8.23 (m, 3H), 8.12 (d, J = 8.7 Hz, 1H), 8.11 – 8.01 (m, 3H), 7.99 (d, J = 8.1 Hz, 2H), 7.72 (ddq, J = 28.6, 14.1, 7.5, 7.0 Hz, 5H), 7.57 (t, J = 7.5 Hz, 2H), 7.42 (d, J = 8.1 Hz, 2H), 7.05 (s, 1H), 4.96 (q, 2H), 2.19 (s, 6H), 1.73 (t, J = 7.0 Hz, 3H) (Figure S4). ^{13}C NMR (151 MHz, $CDCl_3$) δ 179.37, 164.84, 162.53, 160.96, 152.55, 151.58, 138.26, 137.94, 137.76, 133.93, 133.51, 131.70, 130.28, 128.71, 128.64, 127.60, 127.33, 127.10, 126.30, 122.29, 111.60, 53.79, 43.46, 25.33, 14.12 (Figure S5). HR-MS (*m/z*): Calculated for $[C_{28}H_{32}N_4O_5]^+$: 512.2221, found: 512.2285 (Figure S6).

2.2. Detection of CES2 in solution

In the detection of CES2, the probe DBF-CES2 was first dissolved in DMSO to prepare a 1 mM stock solution. A test solution was then prepared by mixing 1 mM DBF-CES2 stock solution, a specific concentration of the analyte, and PBS (10 mM, pH 7.4) to a total volume of 1 mL, and the final concentration of DBF-CES2 in the solution was 10 μM. Enzymatic reaction parameters were optimized to find the optimal test conditions.

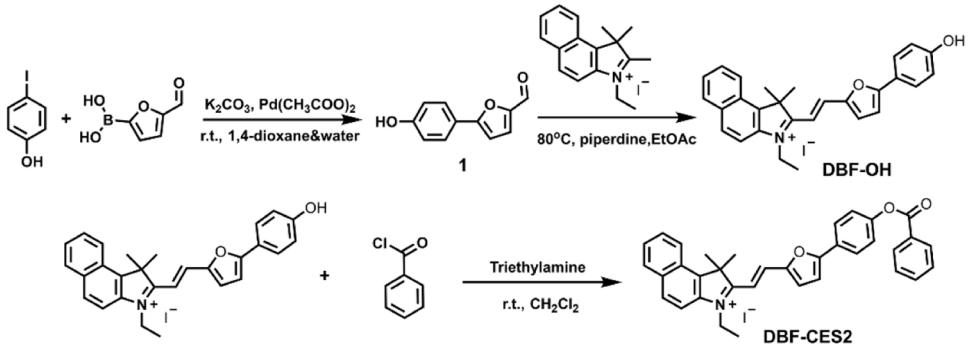

Fig. 1. The synthesis process of DBF-OH and DBF-CES2.

2.3. Cellular imaging experiments

2.3.1. Cellular endogenous CES2 imaging

NCM460 and SW620 cells were incubated with 10 μM DBF-CES2 at a concentration of for different durations, and cellular imaging experiments were subsequently performed.

Detection of CES2 in inflammatory cells: For the control group, SW620 cells were treated with only DBF-CES2 (10 μM) for 90 min. To explore CES2 expression in inflammatory conditions, SW620 cells were first treated with LPS (1 μg/mL) for 16 h, followed by DBF-CES2 (10 μM) for 90 min. Additionally, the effects of an accelerator and a CES2-specific inhibitor were investigated by treating SW620 cells with 5-FU (1 mM) or LPA (1 mM) for 1 h, followed by DBF-CES2 (10 μM) for 90 min.

2.4. In vivo imaging experiments in mice with colitis and colorectal cancer

2.4.1. Ethical compliance

The animal experiments were conducted under the ethical protocols approved by the Institutional Animal Care and Use Committee (IACUC) of Jilin University, with certification from ethical inspection permit number SY202306031.

2.4.2. Nude mouse model of inflammation

Nude mice were subjected to a 7-day regimen of drinking water containing 5 % dextran sulfate sodium (DSS) to induce a colitis mouse model. They were then characterized by weight loss and bloody stools.

2.4.3. Tumor-bearing nude mice

Five-week-old nude mice, free from specific pathogens, were housed individually in ventilated cages and fed with SPF-grade laboratory food and water. A culture medium containing 2×10^7 cells was subcutaneously injected into the mice. Ectopic SW620 tumors were established until the tumor volume reached about 200 mm^3.

2.4.4. Treatment groups

In the diagram, Group 1 represents the inflammation establishment process, Group 2 received 100 μL of 16 mM mesalazine daily for one week, and Group 3 received 100 μL of 16 mM *Coptis chinensis* water daily for one week.

3. Results and discussion

3.1. Probe design and spectral performance

We designed and synthesized a novel NIR fluorescent probe, DBF-CES2, which consists of two components: the fluorescent moiety DBF-OH and a CES2-specific recognition group, the benzoyloxy group. The fluorescent moiety DBF-OH emitted intense red fluorescence, whereas the probe DBF-CES2 with a typical donor-π-acceptor (D-π-A) structure emitted weak fluorescence. This weak fluorescence is likely due to the conjugation of the benzoyloxy group with the hydroxyl group in the

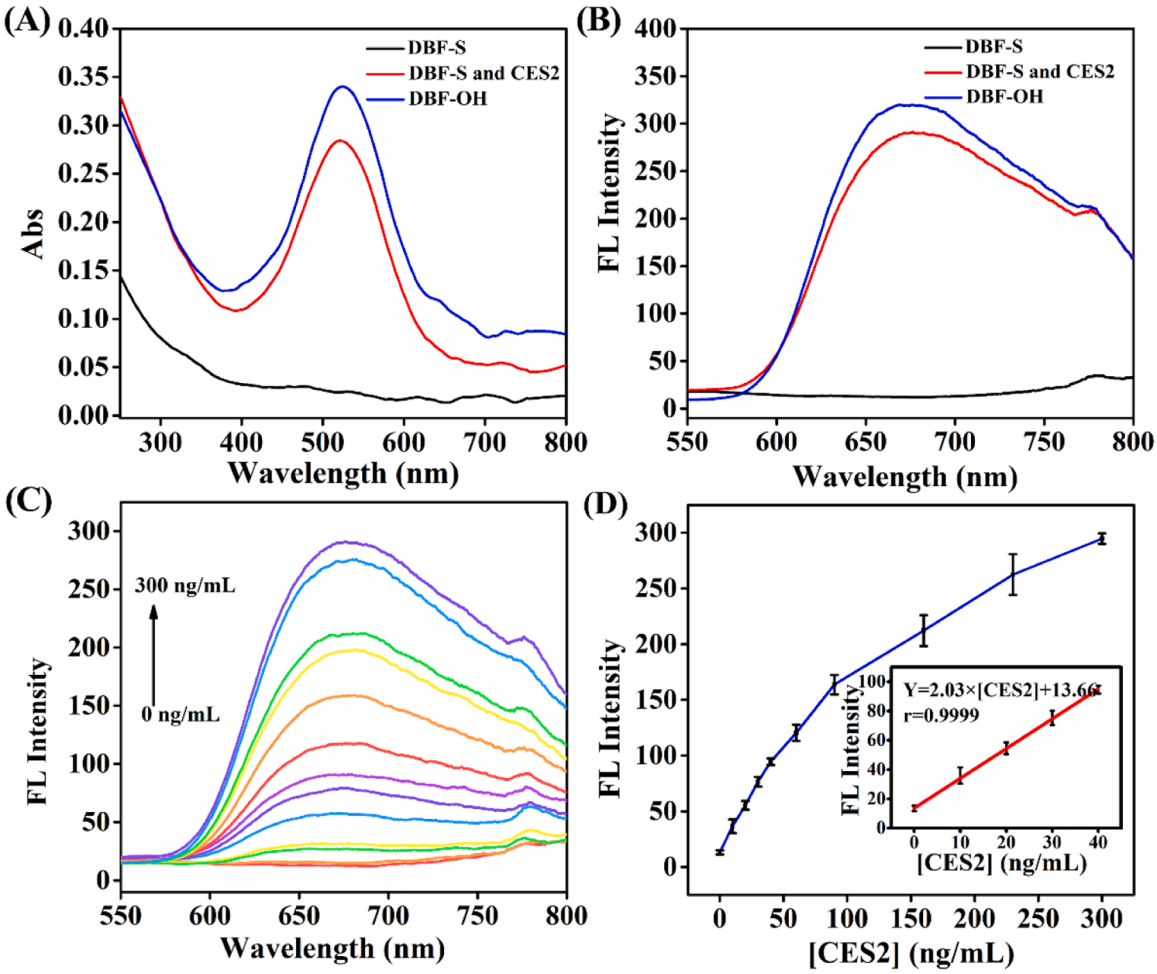

Fig. 2. (A) UV-vis absorption spectra of DBF-CES2 (10 μM), the reaction system and DBF-OH (10 μM). (B) Fluorescence spectra of DBF-CES2 (10 μM), the reaction system and DBF-OH (10 μM); $\lambda_{ex} = 513$ nm. (C) Fluorescence spectra of DBF-CES2 following the gradual addition of CES2; $\lambda_{ex} = 513$ nm. (D) Linear relationship between fluorescence intensity (I_{680}) of DBF-CES2 and CES2 concentration (0–40 ng/mL); $\lambda_{ex} = 513$ nm.

fluorophore, which can reduce the electron donor capacity, in turn inhibiting the intramolecular charge transfer (ICT) process. To explore the spectral performance of the probe in the presence of CES2, we examined the ultraviolet absorption and fluorescence spectra of DBF-CES2 incubated with CES2. As displayed in the ultraviolet absorption spectrum of DBF-CES2 (Fig. 2a), the absorption was nearly unobservable. However, after incubating with CES2, the maximum absorption peak shifted to 520 nm, resulting in a new peak with a significantly increased UV-visible absorption intensity. This new peak aligns with the maximum absorption wavelength of the fluorescent moiety DBF-OH. The fluorescence spectrum of DBF-CES2, depicted in Fig. 2b, was acquired at an excitation wavelength of 513 nm. DBF-CES2 alone emitted weak fluorescence, but upon the addition of CES2, a new fluorescence emission peak emerged at 680 nm. This confirms the formation of a substantial amount of the fluorescent group upon reacting with the enzyme.

Subsequently, molecular docking simulations were conducted to investigate the interaction between the probe DBF-CES2 and CES2. As depicted in Fig. 3, DBF-CES2 formed one hydrogen bond with ARG147 in CES2, in addition to other weak interactions. This indicates a strong binding affinity between the probe and CES2, further corroborated by a low binding energy of −8.2 kcal/mol.

Before conducting all spectral experiments, we investigated the reaction time. The results indicated that the fluorescence intensity of the system increased over time, peaking at 40 min, and no significant increase was observed at 60 min. Thus, 40 min was selected as the optimal reaction time (Figure S7). The fluorescence intensity of DBF-OH increased by approximately 22.6 times as the enzyme concentration was increased (from 0 to 300 ng/mL) (Fig. 2c). This effectively eliminates the interference from the overlapped scattered spectra and self-absorption, thereby enhancing the signal-to-noise ratio of the fluorescence image. Remarkably, the fluorescence intensity at 680 nm showed a strong linear relationship with the enzyme concentration, with r = 0.9999 (Fig. 2d). The detection limit of the probe DBF-CES2 was as low as 0.70 ng/mL, and its Stokes shift was also large with a value of 167 nm. Compared with the detection limits of other CES2 detection probes (Table S1), the detection limit of DBF-CES2 is the lowest. Further, the kinetics of the enzymatic reaction was investigated using the Michaelis−Menten plot and Lineweaver−Burk plot. As shown in Figure S8, V_{max} = 102.77 μM min^{-1} and K_m = 4.0 μM. This demonstrates its feasibility in the fluorescence detection of CES2.

3.2. Optimization of spectral properties of probe DBF-CES2, reaction system, and fluorophore

To investigate its stability under prolonged excitation light irradiation, the fluorescent probe DBF-CES2 was incubated with the sample for extended periods, and its fluorescence intensity at 513 nm was measured every 10 min. As shown in Figure S9, the fluorescence intensity of the system was stable after 50 min of light exposure, with negligible changes thereafter. The fluorescence intensity of both the probe and the fluorophore remained stable under 50 min of being exposed to the excitation light, which indicates the good photostability of the system. With such stability, the probe is unlikely to easily decompose into its fluorescent components, which is beneficial for long-term biological fluorescence imaging applications.

To determine whether DBF-CES2 is suitable for biological detection systems, its response to CES2 at various pH values and temperatures was explored. As depicted in Figure S10, the fluorescence intensity was highest at pH 7.4. Considering that the physiological pH is 7.4, this pH was selected for the final test system. Comparing different temperatures (25 °C, 30 °C, 37 °C, and 42 °C), the system exhibited the highest fluorescence intensity at 37 °C, which aligns with the physiological temperature of biological systems. Therefore, 37 °C was chosen as the

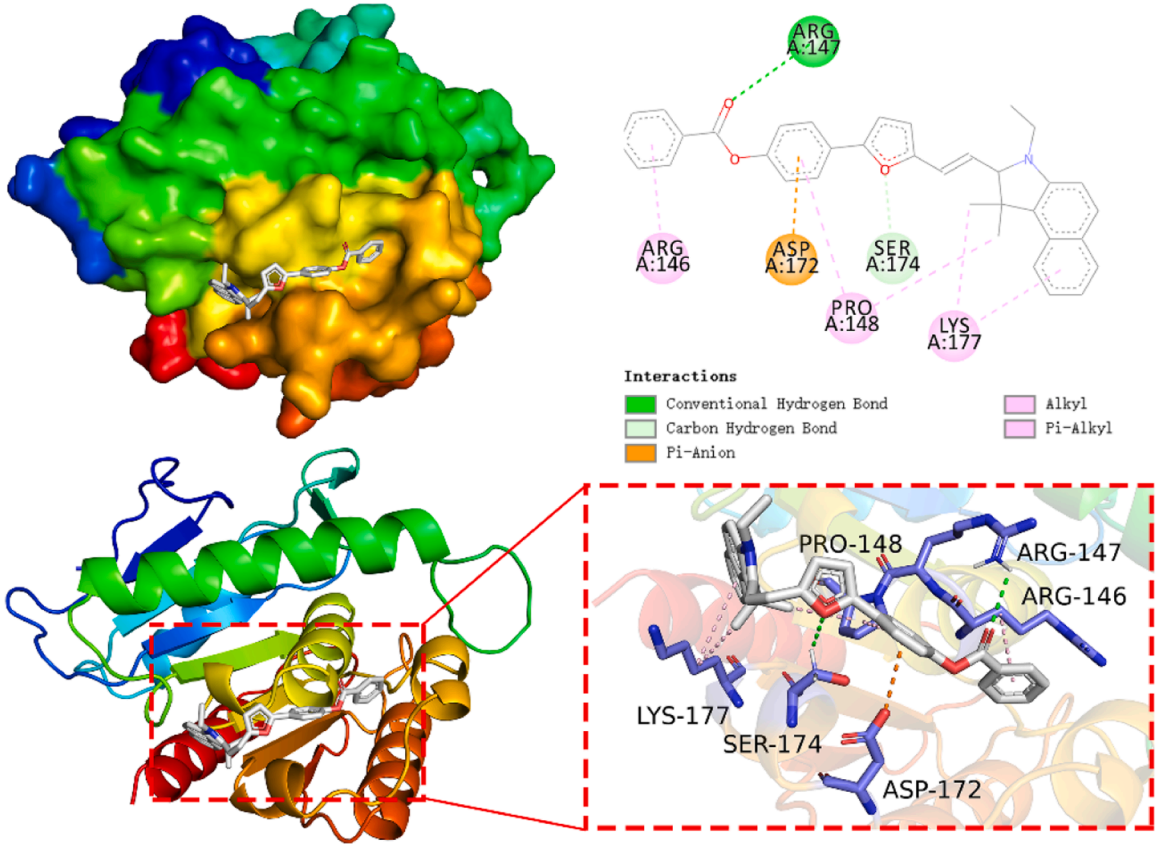

Fig. 3. Molecular docking simulation results showing interactions between DBF-CES2 and CES2.

optimal temperature for the final test system (Figure S11). These optimal conditions align with the physiological environments, which confirms that the method is suitable for subsequent biological experiments. In summary, the optimal *in vitro* experimental conditions were 37 °C, pH 7.4, and 40-minute incubation time.

To evaluate the selectivity of DBF-CES2 towards CES2, 17 common biological substances were tested, including cations, anions, amino acids, and various enzymes. substances were added to a PBS solution containing DBF-CES2, and the fluorescence intensities were measured. As shown in Figure S12, only CES2 elicited a significant response to DBF-CES2, which indicates that the probe has high selectivity and specificity for CES2.

3.3. Cytotoxicity assessment

To explore the relationship between CES2 and normal, colitic, and cancerous cell, this study utilized both normal intestinal cells and colorectal cancer cells for subsequent cellular experiments. Prior to these experiments, the CCK-8 assay was employed to evaluate the cytotoxicity of the normal intestinal cells and colorectal cancer cells to ensure that the probe does not adversely affect cellular health. The feasibility of using this probe in further cellular studies was assessed thereafter. As indicated by the results shown in Figures S13 and S14, after incubating normal intestinal cells and colorectal cancer cells with DBF-CES2 at varying concentrations (0, 10, 20, 30, 50, and 100 μM) for 24 h, cell viability remained above 80 %. This demonstrates that even at higher concentrations, the probe does not compromise cellular health, validating its suitability for subsequent cellular imaging experiments.

3.4. Intracellular endogenous CES2 imaging

The probe DBF-CES2 was utilized to investigate the levels of endogenous CES2 in different cell types. As illustrated in Fig. 4A and B, NCM460 and SW620 cells cultured with DBF-CES2 exhibited red

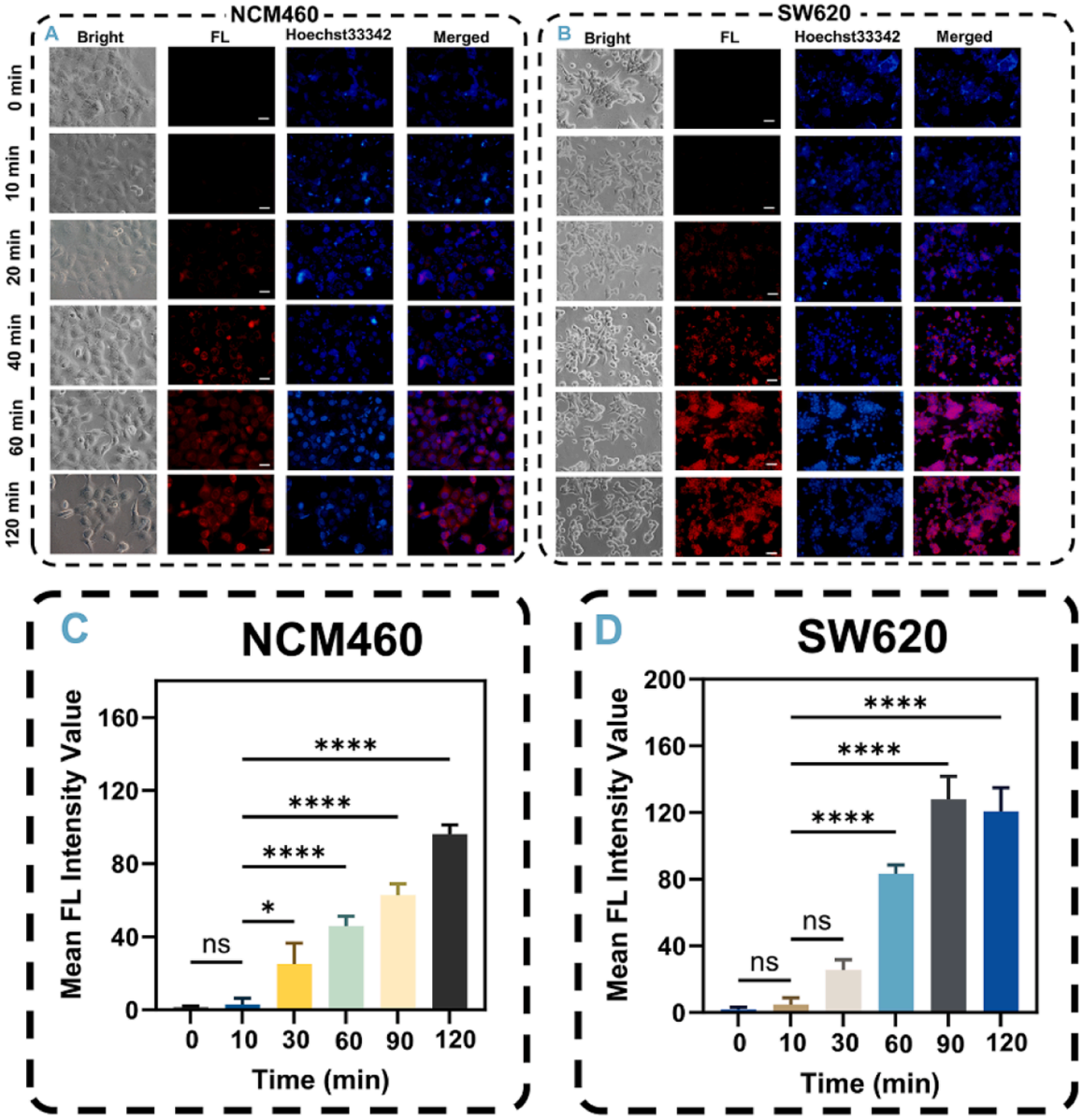

Fig. 4. (A) Sequential fluorescence imaging of DBF-CES2 (10 μM) in NCM460 cells, showing the progression of bright field, fluorescence and hoechst33342 images over time (top to bottom). (B) Sequential fluorescence imaging of DBF-CES2 (10 μM) in SW620 cells, illustrating changes of bright field, fluorescence and hoechst33342 images over time (top to bottom). (C) Averaged intracellular fluorescence intensity of NCM460 cells depicted in (B). (D) Averaged intracellular fluorescence intensity of SW620 cells in (A).

fluorescence. The fluorescence intensity increased over time and reached a plateau at 90 min. This indicates the presence of CES2 in both cell types and suggests that DBF-CES2 has good cell permeability and, thus can penetrate the cell membrane and then enter the cells. Notably, SW620 cells had higher fluorescence intensity, which is indicative of the possible overexpression of CES2 in these cells. These results demonstrate that the probe DBF-CES2 can effectively detect fluctuations in CES2 activity levels within cells and thus can be a valuable tool for monitoring CES2 activity in living cells.

3.5. Detection of CES2 in inflammatory cells

As depicted in Fig. 5, SW620 cells were treated with various agents including 5-FU (a CES2 inducer), the inhibitor LPA, and LPS, and the effects of these agents on CES2 activity were studied. The treatment with 5-FU resulted in the highest fluorescence intensity, which is an indication of an increase in CES2 activity during this process. Conversely, when SW620 cells were treated with LPA, the fluorescence intensity decreased, which is suggestive of a reduction in CES2 content. Additionally, previous studies have reported a close relationship between inflammation and CES2 production. Therefore, SW620 cells were also treated with LPS. The treatment led to a notable decrease in fluorescence signal, an indication of a significant reduction in CES2 expression and activity in inflammatory cells. These results demonstrate that the probe DBF-CES2 is highly sensitive to changes in intracellular CES2 activity and thus has potential in the dynamic monitoring of CES2. The probe DBF-CES2 can also aid in understanding biological activities related to CES2 in organisms. Furthermore, due to its high sensitivity and specificity, DBF-CES2 can serve as a powerful diagnostic tool for inflammation-related diseases and for offering insights into the regulatory mechanisms of CES2 under various pathological conditions.

3.6. Establishment and imaging of colitis and colorectal cancer mouse models

Following the validation of its spectral properties and application in detecting CES2 in cellular experiments, the probe DBF-CES2 had excellent spectral performance, which made it a beneficial imaging tool. To further explore the probe's capability in *in vivo* detection of CES2 in colitis and colorectal cancers, mouse models for the two cancer conditions were established. As shown in Fig. 6 A and 6B, a gradual decline in mouse body weight was observed during the development of colonic inflammation. The treatment of the condition with mesalazine and *Coptis chinensis* water led to the recovery of body weight to a varying degree as the colitis gradually improved.

To validate the differences in CES2 expression among colitis, colorectal cancer, and normal mice, the probe was injected into the mice. Based on the results depicted in Fig. 6C, D, and E, compared to normal mice, the CES2 expression in the colorectal cancer mice was higher whereas that in colitis mice was lower. Additionally, tissue section experiments were conducted to further verify the successful establishment of the models. This provides effective strategies for treating the mouse model of colitis using traditional Chinese medicine like *Coptis chinensis* water and Western medicine like mesalazine. The results from *in situ* imaging of the *Coptis chinensis* water treatment group showed a trend toward fluorescence recovery. Anatomical images of organ tissue sections showed some blank areas compared to normal colon staining; however, the numbers of these areas were significantly lower compared to the inflammation model. This demonstrates the effectiveness of the *Coptis chinensis* water treatment. Similarly, the mesalazine treatment group also showed a trend toward fluorescence recovery, according to the *in situ* imaging. Tissue sections of the treated organs also showed a reduction in blank areas compared to the inflammatory model, which confirms the effectiveness of the mesalazine treatment. These observations are consistent with the aforementioned results on body weight recovery, which strongly suggests that our probe can effectively validate the trends in CES2 expression in colitis and colorectal cancer mouse models and assess the therapeutic effects of the two treatments (Figure S15).

4. Conclusions

In this study, an organic small molecule fluorescent probe, DBF-CES2, was designed and developed for the detection of CES2 activity. The probe DBF-CES2 could specifically recognize CES2, which then triggers the release of the fluorescent moiety DBF-OH, causing the enhancement of the ICT effect, in turn emitting red fluorescence light (λ_{em}=680 nm). The probe had a large Stokes shift (167 nm), high selectivity and sensitivity, and good biocompatibility. Cellular imaging experiments demonstrated that CES2 expression levels in colorectal

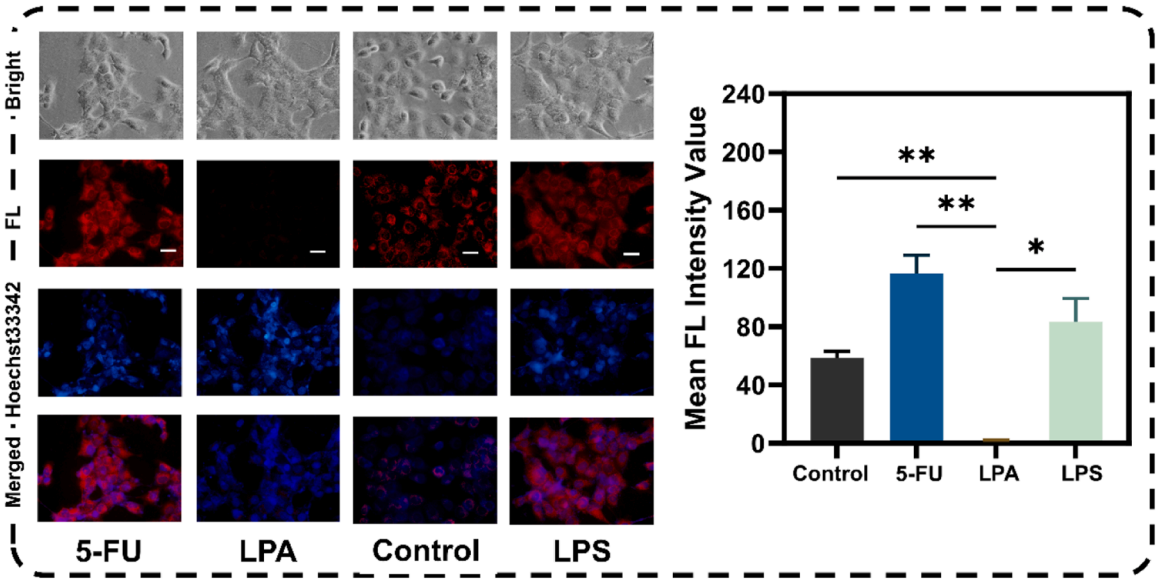

Fig. 5. (A) SW620 cells under different treatments (from left to right): Cells treated with 5-FU (1 mM) for 1 h followed by DBF-CES2 (10 μM) for 90 min; cells treated with LPA (1 mM) for 1 h followed by DBF-CES2 (10 μM) for 90 min; cells treated only with DBF-CES2 (10 μM) for 90 min; and cells treated with LPS (1 μg/mL) for 16 h followed by DBF-CES2 (10 μM) for 90 min. (B) The corresponding averaged intracellular fluorescence intensity of cells in (A).

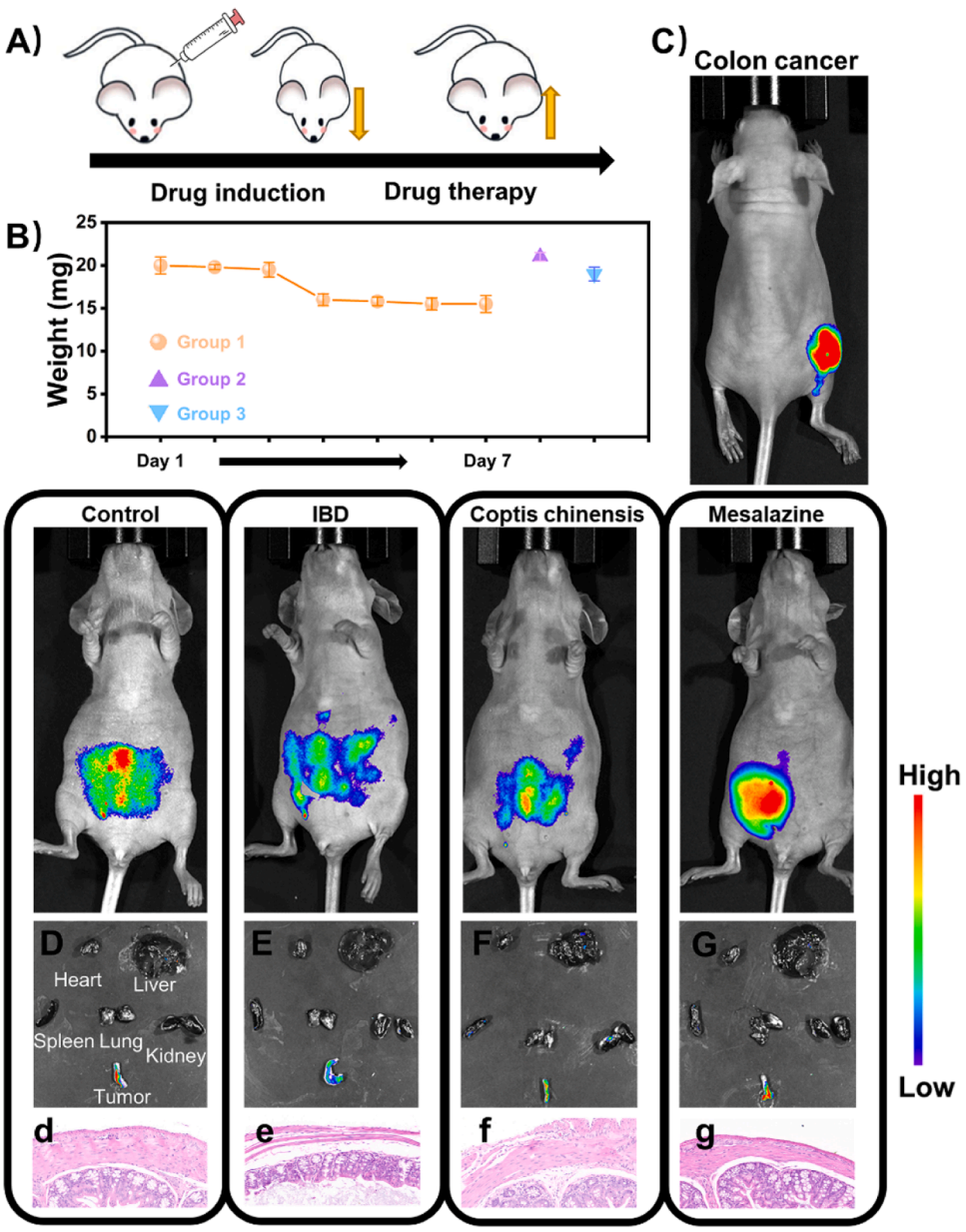

Fig. 6. (A) Schematic diagram showing the establishment of inflammation model and subsequent treatments. (B) Mouse body weight data: G1 represents the body weight during the model establishment process, G2 represents the body weight after treatment with mesalazine, and G3 represents the body weight after treatment with *Coptis chinensis* water. (C) Images of subcutaneous colorectal cancer tumors in mice. (D) *In situ* images and anatomical images of organs for the control group, with (d) showing the H&E staining of the colon pathology. (E) *In situ* images and anatomical images of organs for the IBD group, with (e) showing the pathology of the colon. (F) *In situ* images and anatomical images of organs for the traditional Chinese medicine *Coptis chinensis* water treatment group, with (f) showing the pathology of the colon. (G) *In situ* images and anatomical images of organs for the Western medicine mesalazine treatment group, with (g) showing the pathology of the colon.

cancer cells were higher than those in normal cells, and the DBF-CES2 probe could specifically target endogenous CES2 in colorectal cancer cells; thus, it could easily distinguish between cancerous and normal cells. *In vivo* imaging of mice showed that the probe could easily differentiate between colitis and colorectal cancer and was able to assess the therapeutic effects of two drugs. Overall, the synthesized CES2-targeting organic small molecule fluorescent probe DBF-CES2 is a new molecular tool that can be employed for the early diagnosis of diseases related to colitis and colorectal cancer. It holds a significant potential in clinical diagnostics.

CRediT authorship contribution statement

Xiangqun Jin: Supervision, Resources, Project administration, Funding acquisition. **Pinyi Ma:** Writing – review & editing, Project administration, Funding acquisition, Data curation, Conceptualization. **Daqian Song:** Writing – review & editing, Data curation. **Lihe Zhao:** Writing – review & editing, Validation. **Jingkang Li:** Writing – review & editing, Resources, Investigation. **Siqi Zhang:** Software, Investigation, Formal analysis. **Mo Ma:** Writing – original draft, Validation, Data curation, Conceptualization.

Declaration of Competing Interest

The authors declare that they have no known competing financial interests or personal relationships that could have appeared to influence the work reported in this paper.

Acknowledgments

This work was supported by the National Natural Science Foundation of China (22004046 and 22074052), the Science and Technology Developing Foundation of Jilin Province of China (20230204116YY).

Appendix A. Supporting information

Supplementary data associated with this article can be found in the online version at doi:10.1016/j.snb.2024.137057.

Data Availability

Data will be made available on request.

References

[1] P.T. Santana, S.L. Bittencourt Rosas, B.E. Ribeiro, Y. Marinho, H.S. de Souza, Dysbiosis in inflammatory bowel disease: pathogenic role and potential therapeutic targets, Int. J. Mol. Sci. 23 (2022) 3464.
[2] G.P. Ramos, K.A. Papadakis, Mechanisms of disease: inflammatory bowel diseases, Mayo Clin. Proc. 94 (2019) 155–165.
[3] A. Saez, B. Herrero-Fernandez, R. Gomez-Bris, H. Sanchez-Martinez, J.M. M. Gonzalez-Granado, Pathophysiology of inflammatory bowel disease: innate immune system, Int. J. Mol. Sci. 24 (2023) 1526.
[4] M.T. Alam, G.C.A. Amos, A.R.J. Murphy, S. Murch, E.M.H. Wellington, R. P. Arasaradnam, Microbial imbalance in inflammatory bowel disease patients at different taxonomic levels, Gut Pathog. 12 (2020) 1.
[5] I. Khan, N. Ullah, L. Zha, Y. Bai, A. Khan, T. Zhao, et al., Alteration of gut microbiota in inflammatory bowel disease (IBD): cause or consequence? IBD treatment targeting the gut microbiome, Pathogens 8 (2019) 126.
[6] J. Cosnes, Smoking, Physical Activity, Nutrition and Lifestyle: Environmental Factors and Their Impact on IBD, Dig. Dis. 28 (2010) 411–417.
[7] A.N. Ananthakrishnan, C.N. Bernstein, D. Iliopoulos, A. Macpherson, M.F. Neurath, R.A.R. Ali, et al., Environmental triggers in IBD: a review of progress and evidence, Nat. Rev. Gastroenterol. Hepatol. 15 (2018) 39–49.
[8] L. Di, The Impact of Carboxylesterases in Drug Metabolism and Pharmacokinetics, Curr. Drug Metab. 20 (2019) 91–102.
[9] M.K. Ross, T.M. Streit, K.L. Herring, S. Xie, Carboxylesterases: dual roles in lipid and pesticide metabolism, J. Pestic. Sci. 35 (2010) 257–264.
[10] J. Lian, R. Nelson, R. Lehner, Carboxylesterases in lipid metabolism: from mouse to human, Protein Cell 9 (2018) 178–195.
[11] L. Lan, X. Ren, J. Yang, D. Liu, C. Zhang, Detection techniques of carboxylesterase activity: An update review, Bioorg. Chem. 94 (2020) 103388.
[12] A. Singh, M. Gao, M.W. Beck, Human carboxylesterases and fluorescent probes to image their activity in live cells, RSC Med. Chem. 12 (2021) 1142–1153.
[13] Y.-Q. Song, X.-Q. Guan, Z.-M. Weng, Y.-Q. Wang, J. Chen, Q. Jin, et al., Discovery of a highly specific and efficacious inhibitor of human carboxylesterase 2 by large-scale screening, Int. J. Biol. Macromol. 137 (2019) 261–269.
[14] Z.-M. Weng, G.-B. Ge, T.-Y. Dou, P. Wang, P.-K. Liu, X.-H. Tian, et al., Characterization and structure-activity relationship studies of flavonoids as inhibitors against human carboxylesterase 2, Bioorg. Chem. 77 (2018) 320–329.
[15] L. Xue, X. Qian, Q. Jin, Y. Zhu, X. Wang, D. Wang, et al., Construction and application of a high-content analysis for identifying human carboxylesterase 2 inhibitors in living cell system, Anal. Bioanal. Chem. 412 (2020) 2645–2654.
[16] W. Luo, Q. Diao, L. Lv, T. Li, P. Ma, D. Song, Near-infrared fluorescent probe based on carboxylesterase 2 and viscosity cascade response for early diagnosis of thyroid cancer, Sens. Actuators B-Chem. 412 (2024) 135805.
[17] B. Yang, X. Ding, J. Li, J. Lai, Z. Zhang, X. Xu, et al., Dihydroxanthene-derived fluorescent probe with near-infrared excitation and emission maxima for detecting human carboxylesterase-2 and bioimaging, Sens. Actuators B-Chem. 395 (2023) 134503.
[18] N. Li, W. Yang, R. Liu, Q. Chen, J. Yang, Z. Ni, et al., An innovative near-infrared fluorescent probe designed to track the evolution of carboxylesterase in drug-induced liver injury, Sens. Actuators B-Chem. 402 (2024) 135133.
[19] C. Belthangady, L.A. Royer, Applications, promises, and pitfalls of deep learning for fluorescence image reconstruction, Nat. Methods 16 (2019) 1215–1225.
[20] H. Li, Y. Kim, H. Jung, J.Y. Hyun, I. Shin, Near-infrared (NIR) fluorescence-emitting small organic molecules for cancer imaging and therapy, Chem. Soc. Rev. 51 (2022) 8957–9008.
[21] S. Wang, W.X. Ren, J.-T. Hou, M. Won, J. An, X. Chen, et al., Fluorescence imaging of pathophysiological microenvironments, Chem. Soc. Rev. 50 (2021) 8887–8902.
[22] M.-R. Sun, L.-L. Song, H.-Z. Wei, J.-H. Shi, B. Zhao, T. Tian, et al., Rational construction of a practical enzyme-activatable fluorogenic substrate for hNotum and its applications in functional imaging and inhibitor screening, Sens. Actuators B: Chem. 393 (2023) 134145.
[23] B. Yang, X. Ding, Z. Zhang, J. Li, S. Fan, J. Lai, et al., Visualization of production and remediation of acetaminophen-induced liver injury by a carboxylesterase-2 enzyme-activatable near-infrared fluorescent probe, Talanta 269 (2024) 125418.
[24] Y.-L. Qi, H.-R. Wang, L.-L. Chen, B. Yang, Y.-S. Yang, Z.-X. He, et al., Multifunctional Fluorescent Probe for Simultaneously Detecting Microviscosity, Micropolarity, and Carboxylesterases and Its Application in Bioimaging, Anal. Chem. 94 (2022) 4594–4601.
[25] Y. Shu, C. Huang, H. Liu, F. Hu, H. Wen, J. Liu, et al., A hemicyanine-based fluorescent probe for simultaneous imaging of Carboxylesterases and Histone deacetylases in hepatocellular carcinoma, Spectrochim. Acta Part A-Mol. Biomol. Spectrosc. 281 (2022) 121529.
[26] W. Zhou, Y.-c Liu, G.-j Liu, X.-x Niu, X. Niu, X.-f Li, et al., Water-soluble meso-ester substituted BODIPY with aggregation-induced emission property for ratiometric detection of carboxylesterases in living hepatoma cell, Dyes Pigments 201 (2022) 110189.
[27] S.-Y. Liu, X. Zou, Y. Guo, X. Gao, A highly sensitive and selective enzyme activated fluorescent probe for in vivo profiling of carboxylesterase 2, Anal. Chim. Acta 1221 (2022) 340126.
[28] X. Rong, X. Li, C. Liu, C. Wu, Z. Wang, B. Zhu, Dual-reporter fluorescent probe for precise identification of liver cancer by sequentially responding to carboxylesterase and polarity, Talanta 278 (2024) 126477.
[29] X. Lin, M. Liu, Q. Yi, Y. Zhou, J. Su, B. Qing, et al., Design, synthesis, and evaluation of a carboxylesterase detection probe with therapeutic effects, Talanta 274 (2024) 126060.
[30] N. Li, W. Yang, R. Liu, Q. Chen, J. Yang, Z. Ni, et al., An innovative near-infrared fluorescent probe designed to track the evolution of carboxylesterase in drug-induced liver injury, Sens. Actuators B: Chem. 402 (2024) 135133.
[31] Z.-M. Liu, L. Feng, J. Hou, X. Lv, J. Ning, G.-B. Ge, et al., A ratiometric fluorescent sensor for highly selective detection of human carboxylesterase 2 and its application in living cells, Sens. Actuators B-Chem. 205 (2014) 151–157.
[32] Y. Fan, T. Zhang, Y. Song, Z. Sang, H. Zeng, P. Liu, et al., Rationally Engineered hCES2A near-infrared fluorogenic substrate for functional imaging and high-throughput inhibitor screening, Anal. Chem. 95 (2023) 15665–15672.
[33] Y. Wen, N. Jing, M. Zhang, F. Huo, Z. Li, C. Yin, A space-dependent 'enzyme-substrate' type probe based on 'carboxylesterase-amide group' for ultrafast fluorescent imaging orthotopic hepatocellular carcinoma, Adv. Sci. 10 (2023) 2206681.
[34] J. Li, J. Cao, W. Wu, L. Xu, S. Zhang, P. Ma, et al., A molecular imaging tool for monitoring carboxylesterase 2 during early diagnosis of liver-related diseases, Sens. Actuators B: Chem. 377 (2023) 133122.
[35] X. Tian, F. Yan, J. Zheng, X. Cui, L. Feng, S. Li, et al., Endoplasmic reticulum targeting ratiometric fluorescent probe for carboxylesterase 2 detection in drug-induced acute liver injury, Anal. Chem. 91 (2019) 15840–15845.
[36] L. Wang, L. Wang, X. Sun, L. Fu, M. Sun, X. Wang, et al., Imaging of carboxylesterase 2 expression changes in colitis and colon cancer chemotherapy via a fluorescent probe, Sens. Actuators B-Chem. 409 (2024) 135609.
[37] Y. Wang, F. Yu, X. Luo, M. Li, L. Zhao, F. Yu, Visualization of carboxylesterase 2 with a near-infrared two-photon fluorescent probe and potential evaluation of its anticancer drug effects in an orthotopic colon carcinoma mice model, Chem. Commun. 56 (2020) 4412–4415.
[38] L. Wang, L. Wang, X. Sun, L. Fu, M. Sun, X. Wang, et al., Imaging of carboxylesterase 2 expression changes in colitis and colon cancer chemotherapy via a fluorescent probe, Sens. Actuators B: Chem. 409 (2024) 135609.

Mo Ma is currently a PhD student in School of Pharmacy, Jilin University. His interest is spectral analysis.

Siqi Zhang is currently a PhD student in College of Chemistry, Jilin University. Her interest is spectral analysis.

Jingkang Li is currently a PhD student in College of Chemistry, Jilin University. His interest is spectral analysis.

Lihe Zhao gained her doctor's degree from College of Chemistry, Jilin University in 2022 and she is a senior teacher in Shenzhen Experimental School. His research area is spectral analysis.

Daqian Song gained his doctor's degree from College of Chemistry, Jilin University in 2003 and he is a professor in that school. His research areas are spectral and chromatography analysis.

Pinyi Ma gained his doctor's degree from College of Chemistry, Jilin University in 2017 and he is an associate professor in that school. His research area is spectral analysis.

Xiangqun Jin gained his doctor's degree from College of Chemistry, Jilin University in 2007 and he is a professor in School of Pharmacy, Jilin University. His research areas are spectral analysis and drug analysis.